ENDOR Studies of Pyruvate:Ferredoxin Oxidoreductase Reaction Intermediates

Vladimir F. Bouchev,[†] Cristina M. Furdui,[‡] Saurabh Menon,[‡]
**Rajendra Bose Muthukumaran,[†] Stephen W. Ragsdale,[‡] and John McCracken*,[†]**

Contribution from the Department of Chemistry, Michigan State University, East Lansing, Michigan 48824
and Department of Biochemistry, Beadle Center, University of Nebraska, Lincoln, Nebraska 68588-0664

Abstract: Electron−nuclear double resonance (ENDOR) studies of radical intermediates formed by the oxidative decarboxylation of pyruvate by pyruvate:ferredoxin oxidoreductase were carried out to characterize their electronic structure and elucidate aspects of the recently proposed catalytic mechanism (Menon, S.; Ragsdale, S. W. *Biochemistry* **1997**, *36*, 8484−8494). The EPR spectrum of the PFOR/pyruvate adduct at 4 K displays a narrow resonance centered at $g = 2.008$ that has been attributed to a hydroxyethyl thiamine pyrophosphate (HE-TPP) radical. This spectral feature is superimposed on a broad, complex line shape characteristic of magnetically coupled [Fe$_4$S$_4$] clusters. The ENDOR spectrum at $g = 2.008$ reveals a broad peak with a complex line shape that can be analyzed, assuming that it arises from a composite of two axially symmetric proton hyperfine couplings. The principle coupling values for these two hyperfine tensors were: $A_{||}(1) = 18.9$ MHz, $A_{\perp}(1) = 12.6$ MHz; and $A_{||}(2) = 20.3$ MHz, $A_{\perp}(2) = 14.9$ MHz. The assignment of these features to the methyl protons of the pyruvate substrate was made using isotopic substitution. The temperature independence of these ^{1}H ENDOR line shapes from 4 to 200 K indicates that the methyl group of pyruvate undergoes rapid rotation even at 4 K. The ENDOR spectrum at $g = 2.008$ also shows a pair of derivative peaks centered about the [31]P Larmor frequency that are assigned to a weak hyperfine coupling with the phosphorus nuclei of the TPP cofactor. Two models for the electronic structure of the radical intermediate are discussed. A σ radical model which postulates a pyruvate-derived acetyl-type radical where little unpaired spin density resides on the TPP cofactor, and a π radical model that calls for more extensive delocalization of the unpaired electron spin over the HE-TPP framework. Both models require association of the radical center with the pyrophosphate group of TPP to interpret the observed ^{31}P hyperfine coupling.

Introduction

Pyruvate:ferredoxin oxidoreductase (PFOR) is a member of the 2-keto acid oxidoreductase family, which plays a role in anaerobic fermentative metabolism.[1] The enzyme catalyzes the oxidative decarboxylation of pyruvate with transfer of the acetyl moiety to coenzyme A (CoASH) according to the half-reaction[2]

$$CH_3COCOO^- + CoASH \underset{\xrightarrow{}}{\overset{E_0 = -540\,mV}{\rightleftharpoons}} CH_3COSCoA +$$
$$CO_2 + H^+ + 2e^-$$
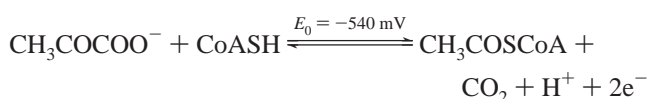
In its function, PFOR is similar to enzymes such as pyruvate dehydrogenase, pyruvate decarboxylase, pyruvate oxidase, and pyruvate:formate lyase, all of which can initiate pyruvate catabolism.

The cofactor content and the mechanism of PFOR remain controversial. Apparently, three prosthetic groups are required for decarboxylation: thiamine pyrophosphate (TPP) and two [Fe$_4$S$_4$] clusters.[3] Recently, Menon and Ragsdale[2] have used a combination of rapid freeze−quench EPR and stopped-flow optical spectroscopy to elucidate and quantify the elementary steps in the reaction mechanism of *Clostridium thermoaceticum*

PFOR. Their data have revealed the presence of a radical intermediate, which has been postulated as a hydroxyethyl thiamine pyrophosphate radical (HE-TPP, see Scheme 1) and proposed as a common transient species in the catalytic reaction of PFORs from different sources. A similar mechanism was proposed earlier by Kerscher and Oesterhelt (1981) for *Hm. halobium* (*Halobacterium salinarium*) PFOR.[4] The catalytic intermediacy of the HE-TPP radical was assumed on the basis of several observations.[2] First, the reaction with pyruvate leads to reduction of a [Fe$_4$S$_4$] cluster with concomitant formation of a radical that exhibits an EPR signal at $g = 2.008$. Second, the radical forms and decays faster than the rate of turnover of the enzyme. Third, the presence of CoA increases the decay rate of the radical by 4400-fold. The observation of electron spin coupling between the radical and at least one of the [Fe$_4$S$_4$] clusters has indicated that the two paramagnetic species are in close proximity (≤ 10 Å).[2,4−6]

For both *Hm. halobium* and *Clostridium thermoaceticum* PFORs, the X-band continuous wave (CW) EPR spectrum of the radical intermediate is centered at $g = 2.00$ and has a peak-to peak line width of approximately 1.8 mT.[2,6] The line shape shows additional features indicative of partially resolved hyperfine structure and is typical for immobilized radicals found

(1) Adams, M. W. W.; Kletzin, A. *Adv. Protein Chem.* **1996**, *48*, 101−180.

(2) Menon S.; Ragsdale S. W. *Biochemistry* **1997**, *36*, 8484−8494.

(3) Zhang, Q.; Iwasaki, T.; Wakagi, T.; Oshima, T. *J. Biochem. (Tokyo)* **1996**, *120*, 587−599.

(4) Kerscher, L.; Oesterhelt, D. *Eur. J. Biochem.* **1981**, *116*, 595−600.

(5) Cammack, R.; Kerscher, L.; Oesterhelt, D. *FEBS Lett.* **1980**, *118*, 271−273.

(6) Kerscher, L.; Oesterhelt, D. *Trends Biochem. Sci.* **1982**, *7*, 371−374.

Scheme 1. Structure of the Putative Hydroxyethylidene-TPP Intermediate Adapted from Ref 2
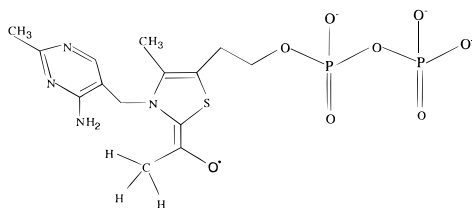
in biological systems. It has also been demonstrated that the EPR line shape of the radical becomes narrower and almost featureless upon substitution of the three protons with deuterons on carbon 3 of pyruvate, showing that the radical species is substrate-derived.[2] Further studies on *Hm. halobium* PFOR by Kerscher and Oesterhelt established a dependency of the EPR line shape of the radical intermediate on the number of protons at the C-3 position of a few 2-oxoacid substrate analogues.[6] The hyperfine pattern has therefore been attributed to interactions between the unpaired electron and the methyl protons of pyruvate.

Unfortunately, inhomogeneous broadening of the EPR line shape prevents the direct measurement of the hyperfine couplings for these protons and precludes the measurement of weaker electron–nuclear couplings that would allow identification of this paramagnetic center as the putative HE-TPP radical species. In this paper, we report the results of X-band electron–nuclear double resonance (ENDOR) experiments on the radical intermediate, providing the first detailed information regarding its electronic structure and proximity to the TPP cofactor.

Experimental Section

Samples of *Clostridium thermoaceticum* PFOR poised with pyruvate or ^2H_3C-labeled pyruvate have been prepared as described previously.[2] After lysing the cells in Tris-HCl buffer, PFOR was purified in MOPS buffer following a procedure given by Wahl and Orme-Johnson[2,7] Metal, sulfide, and protein analysis of the enzyme have shown that it exists as a dimeric protein containing two $[Fe_4S_4]$ clusters per monomer.[2] ^2H_3C-pyruvate was synthesized, following a literature procedure[8] and its purity was found to be greater than 95% by mass spectrometry. The samples were prepared in an anaerobic chamber by reacting a solution containing PFOR (50 μM, final) and TPP (1 mM) with ^1H_3C- or ^2H_3C-labeled pyruvic acid (10 mM, final) at 25 °C in a final volume of 200 μL. The reactions were quenched after 2 min by immersing the tubes in liquid nitrogen.

EPR and ENDOR spectra were recorded on a Bruker ESP 300E spectrometer, equipped with a Bruker ESP 360 DICE ENDOR assembly. An Oxford ESR-900 cryostat and ITC 502 temperature controller were used to maintain constant sample temperature. Electron *g*-values were determined from magnetic field strengths and microwave frequencies measured by a Bruker ER 035M NMR Gaussmeter and an EIP 25B frequency counter, respectively. ENDOR measurements utilized the standard Bruker TM_{110} ENDOR cavity fitted with a home-built removable helix assembly for introducing the radio frequency (rf) radiation.[9] Radio frequency current was amplified by an ENI A-300 power amplifier, and ENDOR spectra were collected in frequency modulation mode by stepping the rf frequency over the range from 0.5 to 35 MHz.

ENDOR simulations were done using FORTRAN-based software written in-house. For ^1H ENDOR analysis, the nuclear spin Hamiltonian

(7) Wahl, R. C.; Orme-Johnson, W. H. *J. Biol. Chem.* **1987**, *262*, 10489–10496.

(8) Seravalli, J. Steady-state and time-dependent relaxation studies of the kinetics of action of lactate dehydrogenase from *Bacillus stearothermophilus*. Ph.D. Dissertation, University of Kansas, Lawrence, KS, 1994.

(9) Bender, C. J.; Sahlin, M.; Babcock, G. T.; Barry, B. A.; Chandrashekar, T. K.; Salowe, S. P.; Stubbe, J.; Lindstron, B.; Petersson, L.; Ehrenberg, A.; Sjoberg, B.-M. *J. Am. Chem. Soc.* **1989**, *111*, 8076–8083.
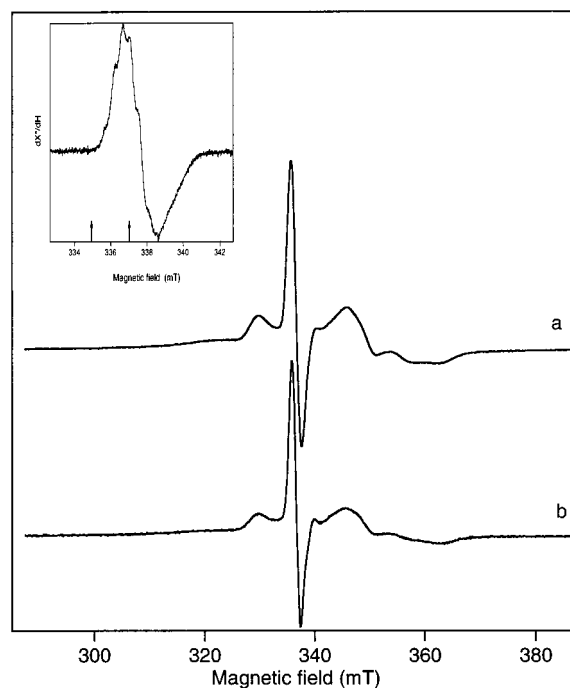

Figure 1. First-derivative EPR spectra of PFOR treated with (a) pyruvate and (b) ^2H_3C-pyruvate. Experimental parameters: field center, 337.6 mT; field sweep width, 100 mT; modulation frequency, 100 kHz; modulation amplitude, 0.5 mT; time constant, 10 ms; microwave power, 0.1 mW; microwave frequency, 9.468 GHz; temperature, 4 K. Inset: Higher resolution spectrum of the $g = 2.00$ region at 60 K. Experimental parameters: field center, 337.72 mT; field sweep width, 10.0 mT; modulation frequency, 100 kHz; modulation amplitude, 0.10 mT; time constant, 10 ms; microwave power, 0.05 mW; microwave frequency, 9.482 GHz. Arrows mark the field positions where ENDOR data were collected.

consisted of nuclear Zeeman and electron–nuclear hyperfine terms. Analytical expressions derived from diagonalization of the Hamiltonian matrix were used along with a standard orientational averaging protocol for randomly ordered samples to obtain an ENDOR spectrum in "absorption mode." Derivative spectra were computed numerically from these powder pattern spectra using the experimental radio frequency FM step size, or "depth," to define the limits for calculating line shape slopes. For ^2H ENDOR simulations, the nuclear quadrupole interaction was included in the spin Hamiltonian and ENDOR frequencies were obtained by numerical diagonalization.

Results

The EPR spectra of samples prepared by the freeze–quench procedure given above, are shown in Figure 1. The intense peak centered at $g = 2.008$, has been assigned to the HE-TPP radical.[2,6] This narrow signal is superimposed on a broad, complex EPR line shape with extrema at $g = 2.046$, $g = 1.948$, and $g = 1.861$. The broad signal is only observed at temperatures below ca. 20 K and has been assigned to the $[Fe_4S_4]$ clusters of the enzyme. The complex line shape of this broad signal deviates from that of a typical rhombic $[Fe_4S_4]$ cluster because of electron spin–spin interactions.[2,10] A higher resolution spectrum of the EPR feature centered at $g = 2.008$ is shown in the inset for PFOR treated with pyruvate prior to freezing. The overall peak-to-peak line width of the signal is 1.93 mT, but the absorbance extends over a range of about 7 mT.

ENDOR spectra of pyruvate-treated PFOR were collected at temperatures ranging from 4 to 200 K, with the maximum ENDOR response being found at 60 K. At $g = 2.008$, the

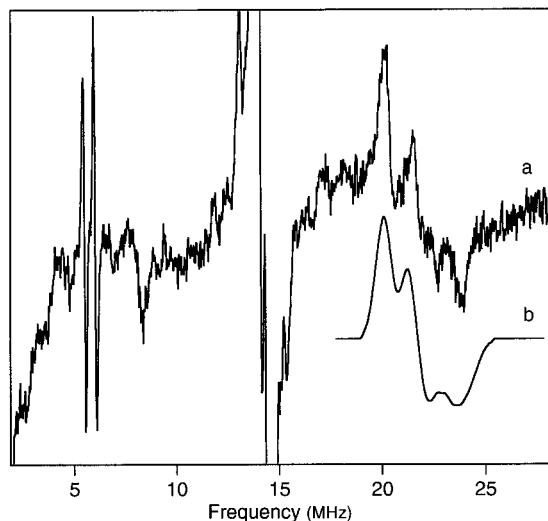(10) Kerscher, L.; Oesterhelt, D. *Eur. J. Biochem.* **1981**, *116*, 587–594.

Figure 2. Wideband ENDOR spectrum of the putative HE-TPP radical collected at $g = 2.010$. Experimental parameters: static magnetic field, 334.1 mT; microwave frequency, 9.400 GHz; microwave power, 10 mW; rf fm modulation depth, 100 kHz; rf power, 220 W; time constant, 10 ms; temperature, 60 K. The data are the average of 100 scans. Inset: (b) Simulated ENDOR spectrum for the high-frequency portion of the proton resonance. Simulation parameters: nuclear g-value, g_n = 5.585; $A_\perp(1) = 12.6$ MHz, $A_\parallel(1) = 18.9$ MHz, $A_\perp(2) = 14.9$ MHz, $A_\parallel(2) = 20.3$ MHz; intrinsic ENDOR line width, 600 kHz; number of θ increments in the range $0-90°$, 360; and the FM modulation depth was set to 100 kHz.

ENDOR spectrum shows a pair of narrow, intense lines at 5.48 and 5.99 MHz, Figure 2. Because these signals are centered at the Larmor precession frequency of ^{31}P (5.75 MHz at 334.1 mT) and the enzyme had never been exposed to phosphate buffer during the purification procedure, they can be assigned to a long-range hyperfine coupling with the phosphorus nuclei of the TPP cofactor. Figure 3 shows the ENDOR spectrum obtained by averaging 300 scans in the narrow frequency range from 3.3 to 8.3 MHz. Both ^{31}P resonances show almost symmetrical derivative line shapes.

The high-frequency region of the spectrum in Figure 2 shows a complex ENDOR powder pattern with features at 20.2, 21.5, 22.6, and 23.8 MHz. On the basis of ENDOR spectra obtained for control samples prepared with ^{2}H$_3$C-pyruvate (see below), these resonances are assigned to strongly coupled protons of the substrate derived HE-TPP moiety. The corresponding low-frequency signals for these peaks should be symmetrically placed about the ^{1}H Larmor frequency (14.2 MHz) and appear at 4.6, 5.8, 6.9, and 8.2 MHz. A negative peak at 8.2 MHz is clearly resolved, and minor features are present at 4.3 and 6.9 MHz. The peak predicted to be at 5.8 MHz is masked by the sharp ^{31}P resonances described above. No significant changes in the observed frequencies and the line shapes of these signals occurred as the temperature was varied from 4 to 200K (Figure 4a–c).

ENDOR experiments were also carried out at $g = 2.02$, 1.98, and 1.93 to check for possible contributions from the reduced [Fe$_4$S$_4$] clusters to the ENDOR spectra collected for the radical at $g = 2.008$. At 60 K, no ENDOR signals were detected other than those shown above for the radical at $g = 2.008$. At 4 K, a broad feature corresponding to matrix protons was resolved at magnetic field strengths corresponding to that of the reduced [Fe$_4$S$_4$] cluster(s). Figure 5 shows the ENDOR spectrum at $g = 2.02$. Absent from these data are the features assigned to ^{31}P and strongly coupled protons that characterized the ENDOR response at $g = 2.008$.
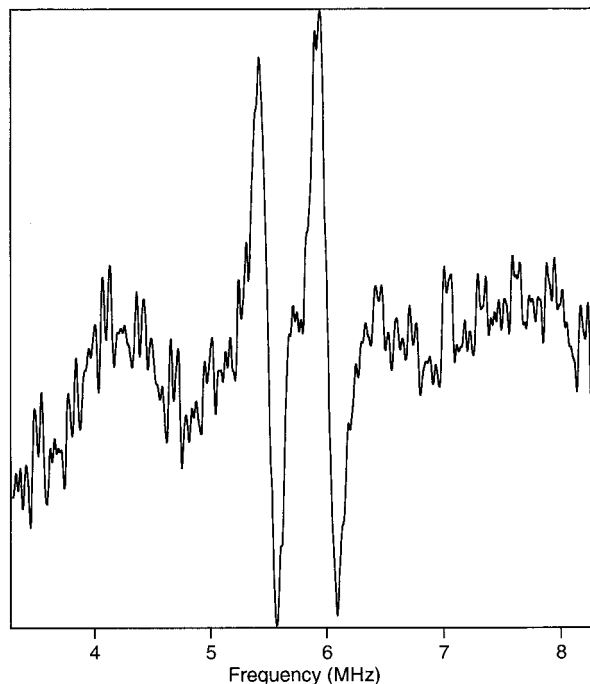

Figure 3. ^{31}P ENDOR spectrum of the putative HE-TPP radical. Experimental parameters: static magnetic field, 334.1 mT; microwave frequency, 9.400 GHz; microwave power, 10 mW; rf sweep width, 5 MHz; rf fm modulation depth, 100 kHz; rf power, 220 W; time constant, 10 ms; sample temperature, 60 K. 300 scans were averaged.

The ENDOR spectrum of PFOR reacted with ^{2}H$_3$C-labeled pyruvate at 60 K, Figure 4d, shows the proton matrix line at 14.2 MHz and the two ^{31}P peaks at 5.48 and 5.99 MHz. The proton lines, observed previously from 19 to 24 MHz, are strongly suppressed with the major contribution being a baseline distortion that was also observed at $g = 2.02$ (Figure 5). A new feature centered at 3.34 MHz was resolved and assigned to the pyruvate-derived methyl deuterons. Figure 6 shows an ENDOR spectrum collected over a narrow frequency range about the deuterium signal. This ^{2}H ENDOR signal has a complex line shape due to the combined effect of nuclear quadrupole and anisotropic hyperfine interactions. A portion of the corresponding low-frequency ^{2}H hyperfine component is also resolved near 1 MHz, but it is distorted by baseline artifacts present in this region and truncated by the scanning limitations of the Bruker DICE ENDOR accessory.

Discussion

The ENDOR data presented here unambiguously show that the EPR signal at $g = 2.008$ corresponds to a substrate-derived catalytic intermediate. The presence of proton ENDOR signals at 20.2, 21.5, 22.6, and 23.8 MHz in the spectrum of pyruvate-treated PFOR and their sensitivity to isotopic substitution of the substrate protons lead to the conclusion that the observed signals are due to the substrate hydrogens. The appearance of corresponding deuteron ENDOR lines upon isotopic substitution supports this conclusion and provides additional constraints for the analysis of the substrate-derived proton hyperfine couplings.

The higher frequency portion of the ^{1}H ENDOR spectrum shown in Figure 3 can be interpreted, assuming that two overlapping powder-type line shapes of axial symmetry contribute equally to the spectrum. The magnitudes of the proton hyperfine couplings were obtained by computer simulation of the ENDOR line shape in the 19–24 MHz region. The insert in Figure 2 shows the simulated high-frequency ENDOR
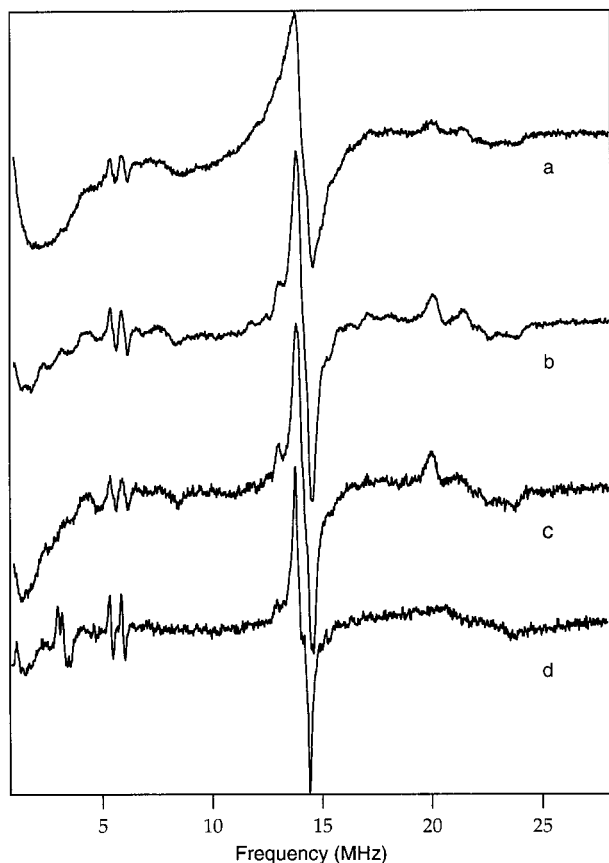
ENDOR Studies of PFOR Reaction Intermediates

J. Am. Chem. Soc., Vol. 121, No. 15, 1999 **3727**

Figure 4. Temperature dependence of the ENDOR spectrum of the PFOR/pyruvate radical EPR signal. Experimental parameters: static magnetic field, 334.1 mT; microwave frequency, 9.400 GHz; microwave power, 20 mW; rf sweep width, 27 MHz; rf fm modulation depth, 280 kHz; rf power, 220 W; time constant, 10 ms; 100 scans were averaged at sample temperatures of (a) 4 K, (b) 77 K, (c) 200 K,. Trace (d) represents the ENDOR spectrum collected at 60K for the HE-TPP radical prepared by adding ^2H_3C-pyruvate to enzyme. Experimental parameters for these data were: static magnetic field, 334.1 mT; microwave frequency, 9.400 GHz; microwave power, 5 mW; rf sweep width, 27 MHz; rf fm modulation depth, 100 kHz; rf power, 220 W; time constant, 10 ms.

Figure 5. Low-temperature ENDOR spectrum of PFOR/pyruvate collected at $g = 2.02$, 25 mT upfield from the center of the HE-TPP radical signal. Experimental parameters: static magnetic field, 332.2 mT; microwave frequency, 9.400 GHz; microwave power, 1 mW; rf sweep width, 27 MHz; rf fm modulation depth, 100 kHz; rf power, 220 W; time constant, 10 ms; sample temperature, 4K; scans averaged, 100.

Figure 6. ENDOR spectrum of PFOR/^2H_3C-pyruvate. Experimental parameters: static magnetic field, 334.1 mT; microwave frequency, 9.400 GHz; microwave power, 5 mW; rf sweep width, 6 MHz; rf fm modulation depth, 100 kHz; rf power, 220 W; time constant, 10 ms; temperature, 60 K. Inset: Simulated ^2H ENDOR powder pattern. Simulation parameters: nuclear *g*-value, $g_n = 0.8574$; $A_\perp(1) = 1.93$ MHz, $A_{||}(1) = 2.90$ MHz, $A_\perp(2) = 2.29$ MHz; $A_{||}(1) = 3.11$ MHz; $e^2qQ = 50$ kHz, $\eta = 0$; intrinsic ENDOR line width, 70 kHz; number of θ increments in the range $0-90°$, 60, number of φ increments in the range $0-90°$, 40.

components for the anisotropic hyperfine interaction of the two sets of protons. The principle values of the two hyperfine tensors used to obtain this simulation were $A_{||}(1) = 18.9$ MHz, $A_\perp(1) = 12.6$ MHz; and $A_{||}(2) = 20.3$ MHz, $A_\perp(2) = 14.9$ MHz. To obtain a simulated powder pattern where the high-frequency negative feature at 23.8 MHz showed an amplitude similar to that of the positive feature resolved at 21.5 MHz, it was necessary to use $A_{||}$ values for the two tensors that differed by 1.4 MHz. The $A_\perp$ values needed to be offset from one another by 2.3 MHz so that the "positive lobes" of both perpendicular features can add to yield the peaks observed at 20.2 and 21.5 MHz.

The two hyperfine tensors extracted from the ENDOR data are thus associated with two sets of substrate-derived methyl protons. The symmetry and magnitude of the anisotropic hyperfine couplings are characteristic of the interaction of an unpaired electron with β-protons. The small difference in the values of the isotropic hyperfine components, 14.7 and 16.7 MHz, indicate that the corresponding sets of β-protons are nearly equivalent. β-couplings of three methyl protons to an unpaired electron would hypothetically give rise to up to eight lines in the EPR spectrum and three pairs of powder line shapes in the ENDOR spectrum, provided that the three protons were non-
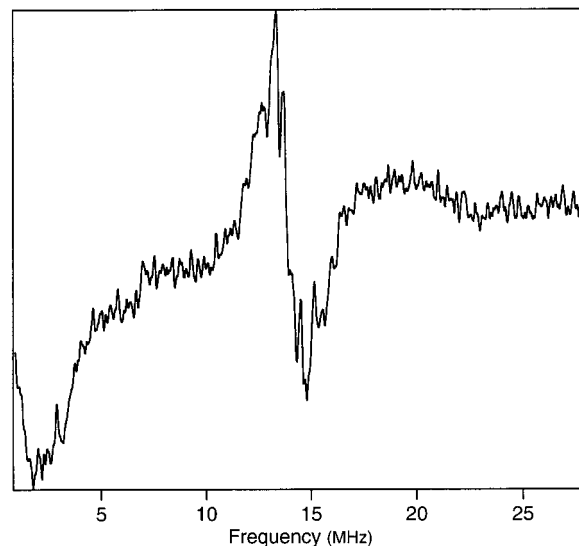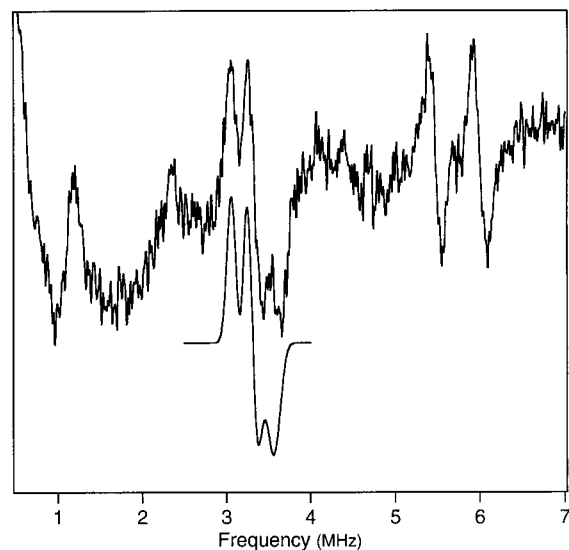
equivalent. Such spectra would be expected at sufficiently low temperatures where rotation of the methyl group is frozen. However, if the internal rotation of the methyl group about the $C_\alpha-C_\beta$ bond is fast enough, so that the frequency of rotation is high in comparison with the hyperfine precession frequency of the protons, the proton couplings will be equalized.[11-13] The EPR spectrum of the methyl group will then consist of a

(11) Gordy, W. In *Techniques in Chemistry, Vol. XV: Theory and Applications of Electron Spin Resonance*; West, W., Ed.; Wiley: New York, 1980; pp 202−229.

1:3:3:1 quartet, while the corresponding ENDOR spectrum will be a single pair of lines with small anisotropy characteristic of β protons.[14,15] This situation is encountered in solutions and even in solids at sufficiently high temperatures. It is well-known that significant rotation of the CH_3-group is present even at temperatures as low as 4.2 K.[11−17] In addition, at low temperatures (e. g., below 77 K) the methyl group may execute restricted rotation through a quantum mechanical barrier tunneling process that exchanges the methyl protons.[18−22]

The detection of only two pairs of proton hyperfine lines in the ENDOR spectrum of pyruvate reacted PFOR cannot be accounted for by the hyperfine effects of a frozen, stationary methyl group. Raising the temperature would eventually lower the potential barrier to the internal rotation and the ENDOR lines for the nonequivalent, frozen protons would collapse into a single pair. However, such effects were not observed in the present study. The invariance of the ENDOR line shapes from the methyl protons of pyruvate with respect to the temperature indicates that the methyl group must be rapidly rotating, even at temperatures as low as 4.2 K. The two pairs of β-proton ENDOR signals that correspond to two sets of almost equivalent methyl protons then should originate from two populations of radical species that differ slightly in their structure, most likely in their conformation. Simulations aimed at interpreting the observed hyperfine powder pattern line shape by considering single anisotropic tensor with a rhombic symmetry were unsuccessful. This model was not able to account for the relative intensities of the powder line shape features for both ^1H and ^2H ENDOR spectra.

Isotopic replacement of the pyruvate methyl hydrogens by deuterium causes the observed ENDOR hyperfine lines to shift to the frequency range about the deuteron Larmor precession frequency (2.18 MHz at 334.1 mT). The hyperfine coupling constants for the two sets of protons reported above are expected to be scaled down by a factor of $g_n(^1H)/g_n(^2H) = 6.51$ upon ^2H substitution. Because ^2H is an $I = 1$ nucleus, the nuclear quadrupole interaction must be included in the Hamiltonian that describes the electron−nuclear coupling. Numerical simulations were done in a manner similar to those for the ^1H ENDOR spectra to demonstrate that the ^1H hyperfine coupling parameters would allow for satisfactory analysis of the ^2H ENDOR signal. Two sets of deuteron spin Hamiltonian parameters, corresponding to those used to simulate the ^1H ENDOR features observed from 19 to 25 MHz, were used as input. The experimental and simulated spectra are shown in Figure 6. The frequencies of the corresponding simulated and experimental peaks agree within 0.05 MHz. The ^2H hyperfine coupling parameters used in the simulation were $A_\parallel(1) = 2.90$ MHz, $A_\perp(1) = 1.93$ MHz, $A_\parallel(2) = 3.11$ MHz and $A_\perp(2) = 2.29$ MHz. A small quadrupole coupling, $e^2qQ/h = 50$ kHz, was necessary to prevent further splitting of the ^2H ENDOR line shape. This upper limit for the quadrupole coupling constant is within the range of reported constants for the quadrupole interaction in organic compounds

with covalently bonded deuterons (30−340 kHz).[20,23−25] The demonstrated conversion of the high-frequency ^1H ENDOR hyperfine coupling parameters into values that simulate the ^2H ENDOR line shape, supports our ^1H ENDOR analysis model.

The hyperfine coupling parameters for the β-proton hyperfine interaction in the PFOR reaction intermediate are very similar to those measured for the protons in polycrystalline acetyl radical ($CH_3 \cdot C=O$).[26] The acetyl radical is relevant to the PFOR-catalyzed reaction because it can potentially emerge as an intermediate during pyruvate decarboxylation. The principal values of the proton hyperfine coupling tensor reported by Bennet and Mile[26] on the basis of their analysis of ^1H and ^{13}C couplings in the EPR spectra of polycrystalline acetyl radical are $A_\perp = 13.0$ MHz and $A_\parallel = 16.9$ MHz, with an estimated overall error of ± 4 MHz. These authors concluded that Ac$\cdot$ was a σ-type radical with a $C_\beta - C_\alpha = O$ bond angle of 130°. Their analysis showed that the unpaired electron was located primarily in a sp^2-hybrid orbital on the carbonyl carbon atom but that there was also an appreciable spin density on the adjacent carbon and on the oxygen atom. The unpaired spin density on the two acetyl carbons, calculated by using the measured values for the principal elements of the ^{13}C axially symmetric hyperfine tensors and the theoretical values of the hyperfine coupling constants for the fully occupied 2s- and 2p-orbitals was found to be 0.27 for the methyl carbon and 0.52 for the carbonyl carbon. Those results suggested that there was a participation of the excited state, expressed by the valence bond structure $[H_3C \cdot + :C=O]$, in the overall electronic structure of the acetyl radical. Such a delocalization of the unpaired electron on the methyl carbon would produce a negative contribution to the hyperfine coupling and would reduce the positive contribution from hyperconjugation. This interplay between two different electronic states accounted for the observation that A_{iso} for the methyl protons of the acetyl group (14.3 MHz) was smaller than the isotropic hyperfine couplings typically measured for methyl protons in other σ and π radicals (usually above 70 MHz).[11,20,27] The smaller magnitudes of the anisotropic hyperfine components for the acetyl radical compared to those observed for a freely rotating methyl group in π radicals ($B_\parallel = 6$ MHz, $B_\perp = -3$ MHz)[27] has been attributed to differences in the spatial configuration and also the lower spin density (0.52) on the carbonyl carbon atom.[26] A comparison of our ENDOR results for the PFOR radical intermediate with those given by Bennet and Mile[26] for the acetyl radical predicts that very little of the unpaired spin density is delocalized over the molecular framework of TPP.

An alternative model that also explains the results of our ENDOR experiments pictures the HE-TPP$\bullet$ species as a π-type radical with a rapidly rotating methyl group. Given this assumption, the unpaired electron spin density at the α carbon atom, $\rho_\pi^{C_\alpha}$, can be obtained using the relationship[11]

(12) Ayscough, P. B. *Electron Spin Resonance in Chemistry*; Methuen: London, 1967; pp 288−290.

(13) Gordy, W. In *Techniques in Chemistry, Vol. XV: Theory and Applications of Electron Spin Resonance*; West, W., Ed.; Wiley: New York, 1980; pp 487−497.

(14) Poole, C. P., Farach, H. A., Eds. *Handbook of Electron Spin Resonance, Data Sources, Computer Technology, Relaxation and ENDOR*; American Institute of Physics: New York, 1994; pp 360−611.

(15) Kevan, L.; Kispert, L. D. *Electron Spin Double Resonance Spectroscopy*; Wiley-Interscience: New York, 1976; pp 199−204.

(16) Heller, C. J. *Chem. Phys.* **1962**, *36*, 175.

(17) Horsfield, A.; Morton, J. R.; Whiffen, D. H. *Mol. Phys.* **1961**, *4*, 425.

(18) Kevan, L.; Kispert, L. D. *Electron Spin Double Resonance Spectroscopy*, Wiley-Interscience: New York, 1976; pp 218−224.

(19) Clough, S.; Poldy, F. *J. Chem. Phys.* **1969**, *51*, 2076−2084.

(20) Clough, S.; Hill, J.; Poldy, F. *J. Phys. C: Solid State Phys.* **1972**, *5*, 518.

(21) Clough, S.; Poldy, F. *J. Phys. C: Solid State Phys.*, **1973**, *6*, 2357.

(22) Rehorek, D.; Hennig, H. *Z. Chem.* **1980**, *20*, 109−110.

(23) Bonera, G.; Rigamonti, A. *J. Chem. Phys.* **1965**, *42*, 175−180.

(24) Glasel, J. A. *J. Am. Chem. Soc.* **1969**, *91*, 4569−4571.

(25) Lucken, E. A. C. *Nuclear Quadrupole Coupling Constants*; Academic Press: New York, 1969; pp 111−117.

(26) Bennet, J. E.; Mile, B. *Trans. Faraday Soc.* **1971**, *67*, 1587−1597.

(27) Ayscough, P. B. *Electron Spin Resonance in Chemistry*; Methuen: London, 1967; pp 227−230, 289−290 and 336−340.

$$A_{\text{iso}\beta,\text{rot}} = \rho_\pi{}^{C_\alpha} Q_\beta \langle\cos^2\theta\rangle$$

where θ is the dihedral angle between the plane containing both the unpaired electron $2\rho_\pi$ orbital and the $C_\alpha-C_\beta$ bond and the plane defined by the $C_\alpha-C_\beta$ and a $C_\beta-H$ bond of the methyl group. For a rotating methyl group, $<\cos^2\theta> = 0.5$, and $Q_\beta = 164$ MHz.[11] The calculated $\rho_\pi{}^{C_\alpha}$ is then 0.168 for species 1 and 0.199 for species 2. This result presents an alternate picture for the HE-TPP radical where most of the spin density is distributed over the rest of the atoms of the conjugated system.

The distance between the H_β nuclear dipole and the C_α electron dipole was calculated using the above unpaired electron populations on the α-carbon atom and the dipolar field value obtained from $A_\parallel$ and $A_\perp$ components:

$$(A_\parallel - A_\perp)/3 = T = \rho_\pi{}^{C_\alpha}g\mu_B g_n\mu_{B,n}/r^3$$

where μ_B and $\mu_{B,n}$ are the electron and nuclear Bohr magnetons, respectively, and r is the electron−nuclear distance in the dipolar approximation. The dipolar distance was found to be 1.95 Å for species 1 and 2.11 Å for species 2. These values are in good correspondence with the molecular geometry average distance of 2.150 Å found between the methyl hydrogens and the carboxyl carbon of H_3CCOOH.[28] The agreement shows that the π radical model is self-consistent and also adequately describes the electronic structure of the radical.

The proposed PFOR intermediate, the HE-TPP radical, is a conjugated system, in which a possible electron delocalization over the thiazole ring can be realized. Preliminary electron spin−echo envelope modulation studies show weak ^{14}N modulations with frequency components between 0.7 and 5.0 MHz being resolved. These modulations may result from unpaired electron spin delocalized onto the thiazole ring of TPP or from peptide or pyrimidine nitrogen[30] hydrogen-bonded to the hydroxy-ethyl oxygen atom. This model is in agreement with the conclusion of Menon and Ragsdale[2] that the HE-TPP radical is not purely oxygen-centered but that there must be significant spin density among a number of atoms in the radical.

Additional evidence that supports delocalization of the unpaired electron spin density over the HE-TPP molecular framework came from attempts to simulate the cw-EPR spectrum of the radical (Figure 1 − inset) using the proton hyperfine couplings measured here. Using an isotropic g-value of 2.008, three protons characterized by $A_\parallel = 20.3$ MHz and $A_\perp = 14.9$ MHz, and an intrinsic EPR line width of 6.5 G, gave rise to simulations characterized by overall peak-to-peak line widths of 1.4 mT. These simulated spectra showed some partially resolved hyperfine structure, but the number of these features was less than that found experimentally (Figure 1 − inset), and their predicted magnetic field positions were incorrect. Taken together, the absence of some of these line shape features in the simple simulations, the failure to adequately describe the width and asymmetry of the HE-TPP radical line shape, and the large intrinsic line width needed to get a better match between experiment and theory indicate that we are far from an adequate description of this paramagnetic intermediate. Additional ENDOR and ESEEM experiments with ^2H- and ^{13}C-labeled pyruvate are currently underway. Higher-field EPR measurements will also be needed to determine the role that g-tensor anisotropy may play in the EPR data.

An interesting feature in the ENDOR spectra of the radical intermediate in the PFOR-catalyzed reaction is the pair of ^{31}P signals. The symmetrical appearance of the derivative line shapes of these signals can only be analyzed by a hyperfine coupling that is dominated by an isotropic interaction. For the spectrum shown in Figure 3, an isotropic coupling of 0.50 MHz with a dipolar interaction of ≤ 0.09 MHz accounts well for the observed peak positions and line shapes. A second model considered for simulation of the ^{31}P ENDOR data called for a hyperfine tensor dominated by a large anisotropic interaction where the two resolved peaks corresponded to perpendicular line shape singularities. This model was unable to yield derivative peaks with positive and negative portions of nearly equal intensity like those observed for PFOR.

The measured ^{31}P isotropic hyperfine coupling corresponds to a very modest amount of unpaired spin density, 5×10^{-5}, being delocalized to the coupled phosphorus atom of the TPP cofactor. This delocalization probably occurs through the thiazole ring and ethylene bridge to the pyrophosphate group (Scheme 1). The anisotropic portion of the coupling is also small, ≤ 0.09 MHz, and commensurate with a point dipole−dipole distance of more than 7.0 Å. This long dipolar distance is in line with the recent results of X-ray crystallographic studies of pyruvate decarboxylase[31] where modeling of the 2-(1-hydroxyethyl) thiamine diphosphate catalytic intermediate shows that the sulfur atom of the thiazole ring is likely the point of significant unpaired electron spin density that lies closest to the diphosphate group. The estimated dipole−dipole distance for that interaction was found to be greater than 6.0 Å.

Conclusion

The ENDOR results obtained in this study provide insight into the structure and magnetic properties of the radical intermediate that arises upon addition of substrate pyruvate to PFOR. The data show unambiguously that the EPR signal detected at $g = 2.00$ is due to a substrate-derived radical. The results can be explained within the framework of two models for the electronic structure of the intermediate. The σ-type radical model postulates a pyruvate-derived acetyl-type radical where little unpaired spin density resides on the TPP cofactor. The π radical model adopts the proposed HE-TPP radical as the reaction intermediate, and calls for more extensive delocalization of the unpaired electron spin. Both models require close association of the radical center with the pyrophosphate group of TPP.

Future high-frequency ENDOR, ESEEM, and higher-field EPR studies of PFOR reacted with ^{13}C-labeled substrate are necessary to allow for an independent determination of the unpaired spin densities on the C-2 and C-3 carbons of pyruvate and an unambiguous assignment of an electronic structure to the radical intermediate.

(28) Tabor. W. J. *J. Chem. Phys.* **1957**, *26*, 974−975.
(29) Ayscough, P. B. *Electron Spin Resonance in Chemistry*; Methuen: London, 1967; pp. 347−348.
(30) Lobell, M.; Crout, D. H. G. *J. Am. Chem. Soc.* **1996**, *118*, 1867−1873.

(31) Dobritzsch, D.; Konig, S.; Schneider, G.; Lu, G. *J. Biol. Chem.* **1998**, *273*, 20196−20204.